

Integrated Flight Simulation of Ascent and Descent Phases of Sub-Orbital Winged Body Reusable Launch Vehicle Mission using Object Oriented Approach

N. Ramesh, V. Krishna Kumar**, S Swaminathan#, Madan Lal®*

**Scientist/Engineer, Launch Vehicle Design Entity(LVDE), Vikram Sarabhai Space Centre(VSSC),INDIA*

***Ex-Scientist/Engineer, LVDE, VSSC, INDIA*

#Group Director, Launch Vehicle Design Group, VSSC, INDIA

®Deputy Director, LVDE, Vikram Sarabhai Space Centre, INDIA

Abstract

This paper gives an overview of modeling, formulation and implementation of different systems for the flight simulation of reusable launch vehicle from lift off to touch down. Modeling and formulation includes the dynamic motion of a space vehicle consisting of three degrees of freedom for translation dynamics and three degrees of freedom for rotational dynamics representing the rigid body attitude movements. Flight simulation software is developed using Object Oriented Programming (OOP) approach. The simulation software integrates the various mathematical models such as earth, propulsion, aerodynamics, navigation, guidance, autopilot, control plant etc. All these models are treated as individual classes that will maintain its objects and related vehicle data. In this paper results of the flight simulation of a sub-orbital Winged Body Re-entry Vehicle (WBRV) from lift off to touch down with wind disturbances are presented. The results cover the mission profile, control force requirements for WBRV mission.

1. Introduction

The demand of reduction in overall launch cost of launch vehicles leads to the research and development of new space transportation vehicles, which call for sophisticated simulation and optimisation software tools. Flight Simulation plays an important role in developing new space vehicles. Flight Simulation is useful for the dynamic analysis, control law design and validation, guidance and trajectory studies, which involve the modelling of the dynamic behaviour of the flight vehicle¹. A sub-orbital Winged Body Re-entry Vehicle (WBRV) is the first step towards realizing the goal of a reusable first stage of two stages to orbit (TSTO) mission. Typically, the first stage of a TSTO vehicle is a winged body, and it requires mastering and understanding of different technologies before going for the actual mission. The proposed re-entry technology demonstrator will be boosted by a solid rocket motor in ascent phase. After the booster burns out the vehicle flies without power till dynamic pressure reaches less than 2kPa. Then the booster will be separated and WBRV will climb to a peak altitude of 65 to 70km and subsequently it follows a high angle of attack un-powered controlled descent during the hypersonic descent phase. WBRV mission includes different flight phases such as lift-off, ascent, coasting, hypersonic to subsonic descent and landing phases. The ascent and descent phase flight imposes several limits on thermal and structural loads on the vehicle and controllability aspects of the vehicle². Software with acronym SANCHAR (Software for Integrated flight simulation of ascent and hypersonic re-entry phases using object oriented approach) is developed for WBRV flight simulation. SANCHAR is capable of simulating the different flight phases of WBRV mission.

1.2 Object oriented design

Flight simulation is very much data sensitive so that the qualitative analysis of data is difficult. Therefore object-oriented framework will help in merging the data and related communication with data for better presentation to the user. Flight simulation software is developed using C++ language and it exploits the features of Object Oriented Programming (OOP) such as polymorphism, inheritance, encapsulation, and abstraction³. The software design allows a system to be viewed as a collection of objects and the interaction between these objects. For different mathematical operations such as vector, quaternion and matrix multiplication, addition, subtraction and the concept of operator overloading are implemented for the different classes. Inheritance defines a relationship between classes wherein one class shares the behaviour of another class. This feature is used for the aerodynamic class where the behaviour of

control surface class is derived from the basic aerodynamics class. The simulation software integrates the various mathematical models representing earth, propulsion, aerodynamics, navigation, guidance, autopilot and control plant (figure 1).

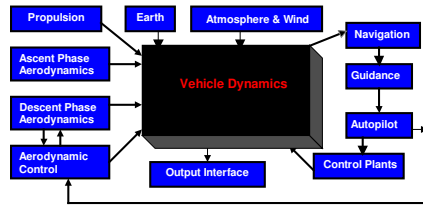


Figure 1 : Flight simulation model

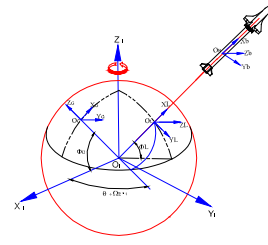


Figure 2 : Co-ordinate Systems

2. Coordinate systems

Coordinate systems and the method in which they are described vary to a great extent depending on the application and the preference of the user. The important coordinate systems used are shown in **figure 2**. Reference frames considered are right handed and cartesian.

2.2 Earth Centred Inertial (ECI) Frame: $OI - X_I Y_I Z_I$

This frame is frozen at launch epoch and origin at the centre of the earth, Z_I axis is along the spin axis of Earth and is positive along the line joining the centre of Earth and North Pole, X_I axis along the intersection of Greenwich meridian at launch epoch and the equatorial plane and Y_I axis completes the right-handed triad.

2.3 Launch Point Inertial (LPI) Frame: $OL - X_L Y_L Z_L$

This frame is frozen at launch epoch and origin is at the launch point, X_L axis along the local vertical and is positive up, Z_L axis along the direction of the launch azimuth in the local horizontal plane, Y_L axis completes the right-handed triad.

2.4 Geographic (GG) Frame: $OG - X_G Y_G Z_G$

Origin is on the surface of the earth at the vehicle's current geocentric latitude and longitude, X_G axis is in local horizontal plane and points north, Y_G axis points east in the horizontal plane through the origin, Z_G axis completes the right-handed triad.

2.5 Body (BODY) Frame: $OB - X_B Y_B Z_B$

Origin is on the longitudinal axis of the vehicle at the instantaneous centre of gravity. X_B is in the plane of symmetry of the vehicle and is positive in the forward direction. Y_B is normal to plane of symmetry and positive towards starboard wing and Z_B axis completes the right-handed co-ordinate system.

2.6 Stability Axis System (Aero): $- X_S Y_S Z_S$

Origin is on the longitudinal axis of the vehicle at the instantaneous centre of gravity. X_S is in the plane of symmetry of the vehicle and along the projection of the vehicle velocity vector on the plane of symmetry and is positive in the forward direction, Y_S axis is along a line normal to the plane of symmetry and is positive to the right looking in the positive X_S direction. Z_S completes the right-handed triad.

3. Equations of motion

The motion of the rigid vehicle can be divided into the motion of the center of mass (CM) and one around this CM^{4&5}. The equations for the motion of CM give information about position and velocity in three directions. The motion around the CM is described by the equations of rotational motion resulting in information on the body rates

around the body axis and the attitude angles of the body. These complete set of equations are called six-degree of freedom equations. These equations can be decoupled into the force and moment vector equations. For simulation force equations are expressed in inertial frame and moment equations in rotating body fixed frame.

$$F = \frac{d(m\bar{V})}{dt} \quad (1) \quad \bar{V} = \{u, v, w\} \quad (2) \quad M = \frac{d\bar{H}}{dt} + \omega \times \bar{H} \quad (3)$$

$$\omega = \{p, q, r\} \quad (4) \quad \bar{H} = [I]\omega \quad (5)$$

Here $[I]$ is the inertia tensor and ω is the angular velocity vector of the body axis system with respect to inertial space and \bar{H} is the angular momentum about C.G. F is the external applied force and M is the external applied moment

$$F = F_{\text{Aero}} + F_{\text{Gravity}} + F_{\text{Main thrust}} + F_{\text{RCS}} \quad (6) \quad M = M_{\text{Aero}} + M_{\text{Main thrust}} + M_{\text{RCS}} \quad (7)$$

Using equations 1,3 & 5 the force and moment equations can be represented as

$$\frac{dV}{dt} = \frac{F}{m} \quad (8) \quad \frac{d\omega}{dt} = [I]^{-1}M + [I]^{-1}(\omega \times ([I]\omega)) \quad (9)$$

These non-linear, coupled differential equations can be integrated in time. The equations of motion are solved by numerical integration methods such as fourth order RK method and Euler method.

3.2 Kinematic equations

Euler angles

The vehicle orientation in space is defined by its attitude, which may be specified in a number of ways. The most common method is to define a sequence of three angles, known as Euler attitude angles. The angular velocity of the vehicle can be expressed as the sum of time derivative components of attitude angles (ϕ, θ, ψ) . The body rates can be obtained by the integration of the equations.

$$d\phi/dt = p + q \sin\phi \tan\theta + r \cos\phi \tan\theta; \quad d\theta/dt = q \cos\phi - r \sin\phi; \quad d\psi/dt = q \sin\phi \sec\theta + r \cos\phi \sec\theta \quad (10)$$

Quaternion

To get the attitude of the vehicle alternative to the use of Euler angles, quaternion representations can be followed⁶. This representation will avoid the singularity when the second rotational angle of Euler representation reaches 90 deg. For the present case quaternion representations are followed. The orientation of the vehicle with respect to a reference frame at any instant in terms of quaternion is defined by

$$\dot{q} = \frac{1}{2}[E]\omega \quad (11)$$

$$q = \{q_0, q_1, q_2, q_3\} \quad [E] = \begin{bmatrix} -q_1 & -q_2 & -q_3 \\ q_0 & -q_3 & q_2 \\ q_3 & q_0 & -q_1 \\ -q_2 & q_1 & q_0 \end{bmatrix}$$

Where q is the vector of quaternion parameters. $[E]$ is the quaternion matrix. The behaviour of the vehicle in flight can be understood by solving the above equations.

3.3 Earth model

Earth is considered as an oblate spheroid (**figure 3**). Let r_i be the position vector of the vehicle in ECI frame.

$$\text{Geocentric latitude } \phi = \sin^{-1}\left(\frac{Z}{r_i}\right) \quad \text{Geodetic latitude } \phi_D = \tan^{-1}\left(\left(R_E / R_p\right)^2 \tan \phi\right) \quad (12)$$

$$\text{Radius of earth at } \phi \quad R_\phi = \frac{R_E}{\left(1 + \left(\left(R_E / R_p\right)^2 - 1\right) \sin^2 \phi\right)^{1/2}} \quad \text{Vehicle's altitude } h = r_i - R_\phi \quad (13)$$

Table 1: Earth model details

R_E	6378137 m
f	0.33528132e-02.
Ω_E	0.7292115e-04 rad/s
R_P	$R_E (1-f)$.
μ	398600.448e+09 m ³ /s ²
J_2	1.0826268e-03

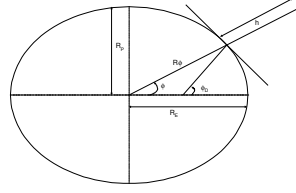


Figure3 : Earth model

Longitude is
$$\theta = \tan^{-1} \left(\frac{Y_I}{X_I} \right) - \Omega_E t \quad (14)$$

The gravity acceleration components in ECI frame are computed as

$$\begin{aligned} G_{XI} &= -\mu (X_I / r_I^3) [1 + 1.5 J_2 (R_E / r_I)^2 \{1 - 5(Z_I / r_I)^2\}] \\ G_{YI} &= -\mu (Y_I / r_I^3) [1 + 1.5 J_2 (R_E / r_I)^2 \{1 - 5(Z_I / r_I)^2\}] \\ G_{ZI} &= -\mu (Z_I / r_I^3) [1 + 1.5 J_2 (R_E / r_I)^2 \{3 - 5(Z_I / r_I)^2\}] \end{aligned} \quad (15)$$

3.4 Atmosphere and Wind

The tables of pressure, temperature and density as a function of altitude are provided for defining the atmosphere model. Indian Standard Atmosphere is used for the flight simulation. Wind model is defined as meridional and zonal components of wind velocity in Geographic (GG) frame as a function of altitude. The wind velocity ($\overline{V_{WI}}$) is transformed to the ECI frame. The relative velocity of the vehicle in ECI frame is $\overline{V_{AI}} = \overline{V_I} - \overline{\Omega_E} \times \overline{r_I} - \overline{V_{WI}}$ and it is transformed to body frame as $V_{AB}(V_{ABX}, V_{ABY}, V_{ABZ})$ for the aerodynamic computations.

Pitch & Yaw angle of attack
$$\alpha = \tan^{-1} \left(\frac{V_{ABZ}}{V_{ABX}} \right) \quad \beta = \sin^{-1} \left(\frac{V_{ABY}}{V_{AB}} \right)$$

3.5 Propulsion Model

Vacuum thrust, propellant mass and consumable mass consumption history is given in tabular form as a function of burn time for solid booster. For simulation, the propellant and consumable masses are interpolated from tables. The vacuum thrust is corrected for atmospheric corrections and the propulsion model takes care of mounting misalignments, canting and thrust misalignments on thrust direction and action point. The propulsion forces and moments considered are due to thrust, jet damping and engine inertia. Jet damping force and moments depends on the mass flow rate and vehicle angular velocity vector. The force and moments are computed as follows.

$$\text{Jet damping force } F_j = -\dot{m} \omega \times r_i \quad (16) \quad \text{Jet damping Moment } M_j = r_i \times F_j \quad (17)$$

Where r_i is a vector representing the thrust location in body frame.

3.6 Mass, C.G and Moment of Inertia

Variation of C.G from reference point and offset along pitch and yaw axis, moment of Inertia and the product of inertia about the axis of body frame along with flight time and mass are provided in a tabular form. The inertia and C.G data will be interpolated for the current flight time based on instantaneous mass that is used for the integration of the rotational equations.

3.7 Aerodynamic model

An important aspect of developing simulation model is the formulation of aerodynamic model. The accuracy of aerodynamic model depends on the degree to which the aerodynamic model represents the physics of the problem. Therefore it is important that all the aerodynamic and control variables that may have influence on the given

$$F_{aero} = QS_{ref} \begin{Bmatrix} -C_D \\ C_S \\ -C_L \end{Bmatrix} \quad \text{Transformation to body frame } F_{Aero \text{ Body}} = [T_{aero \text{ to body}}] F_{aero} \quad (23)$$

All the force coefficients are functions of Reynolds number and Mach number. The non-dimensional aerodynamic force and moment coefficient vary nonlinearly with flow angles (α, β), Mach number and control deflections. Aerodynamic force coefficients are the following,

$$C_{L_{Total}} = C_{L_{Basic}} + \Delta C_{L_{ie}} + \Delta C_{L_{oe}} + \Delta C_{L_{bf}} + \Delta C_{L_{r_left}} + \Delta C_{L_{r_right}} + \Delta C_{L_a} + \Delta C_{L_q} + \Delta C_{L_{flex}} + \Delta C_{L_{lg}} + \Delta C_{L_{ge}} \quad (24)$$

$$C_{D_{Total}} = C_{D_{Basic}} + \Delta C_{D_{ie}} + \Delta C_{D_{oe}} + \Delta C_{D_{bf}} + \Delta C_{D_{r_left}} + \Delta C_{D_{r_right}} + \Delta C_{D_{flex}} + \Delta C_{D_{lg}} + \Delta C_{D_{ge}} + \Delta C_{D_{JET}} + \Delta C_{D_q} + \Delta C_{D_a} \quad (25)$$

$$C_{S_{Total}} = C_{S_{Basic}} + \Delta C_{S_{ie}} + \Delta C_{S_{oe}} + \Delta C_{S_{bf}} + \Delta C_{S_{r_left}} + \Delta C_{S_{r_right}} + \Delta C_{S_p} + \Delta C_{S_r} + \Delta C_{S_{flex}} + \Delta C_{S_{lg}} + \Delta C_{S_{ge}} \quad (26)$$

Where the subscripts represents the following,

bf – body flap, r_left & r_right – left and right rudder, $flex$ – flexibility effect, lg -landing gear, ie & oe – inner & outer elevon, ge – ground effect

Aero Moment Coefficients

Since gravity force acts through C.G it does not generate any moments about it. Aerodynamic moments about C.G are represented in body axis system because the moments of inertia of the vehicle are reasonably constant in body axes. Therefore angular accelerations are easier to formulate in body axis.

$$\frac{d\omega}{dt} = [I]^{-1} M + [I]^{-1} (\omega \times ([I]\omega)) \quad (27)$$

Where $M = M_{Aero} + M_{Thrust} + M_{RCS}$

The components of aerodynamic moments about C.G in body axes are given by $\{l_{cg}, m_{cg}, n_{cg}\}$.

$$M_{Aero} = \begin{Bmatrix} l_{cg} \\ m_{cg} \\ n_{cg} \end{Bmatrix} = \bar{q} S_{ref} \begin{Bmatrix} bC_{l_{cg}} \\ cC_{m_{cg}} \\ bC_{n_{cg}} \end{Bmatrix} + \begin{Bmatrix} l_{RCS} \\ m_{RCS} \\ n_{RCS} \end{Bmatrix} \quad \text{Where } C_{l_{cg}}, C_{m_{cg}}, C_{n_{cg}} \text{ - roll, pitch and yaw moment coefficients.}$$

Aerodynamic moment coefficients are:

$$C_{m_{cg}} = C_{m_{cg \text{ Basic}}} + \Delta C_{m_{cg \text{ ie}}} + \Delta C_{m_{cg \text{ oe}}} + \Delta C_{m_{cg \text{ bf}}} + \Delta C_{m_{cg \text{ } \delta r_left}} + \Delta C_{m_{cg \text{ } \delta r_right}} + \Delta C_{m_{cg \text{ } \alpha}} + \Delta C_{m_{cg \text{ } q}} + \Delta C_{m_{cg \text{ } \dot{q}_{bf}}} + \Delta C_{m_{cg \text{ } flex}} + \Delta C_{m_{cg \text{ } lg}} + \Delta C_{m_{cg \text{ } ge}} \quad (28)$$

$$C_{n_{cg}} = C_{n_{cg \text{ Basic}}} + \Delta C_{n_{cg \text{ ie}}} + \Delta C_{n_{cg \text{ oe}}} + \Delta C_{n_{cg \text{ bf}}} + \Delta C_{n_{cg \text{ } \delta r_left}} + \Delta C_{n_{cg \text{ } \delta r_right}} + \Delta C_{n_{cg \text{ } \beta}} + \Delta C_{n_{cg \text{ } p}} + \Delta C_{n_{cg \text{ } r}} + \Delta C_{n_{cg \text{ } flex}} + \Delta C_{n_{cg \text{ } lg}} + \Delta C_{n_{cg \text{ } ge}} \quad (29)$$

$$C_{l_{cg}} = C_{l_{cg \text{ Basic}}} + \Delta C_{l_{cg \text{ ie}}} + \Delta C_{l_{cg \text{ oe}}} + \Delta C_{l_{cg \text{ bf}}} + \Delta C_{l_{cg \text{ } \delta r_left}} + \Delta C_{l_{cg \text{ } \delta r_right}} + \Delta C_{l_{cg \text{ } p}} + \Delta C_{l_{cg \text{ } r}} + \Delta C_{l_{cg \text{ } flex}} + \Delta C_{l_{cg \text{ } lg}} + \Delta C_{l_{cg \text{ } ge}} \quad (30)$$

Where the subscripts represents the following,

bf – body flap, r_left & r_right – left and right rudder, $flex$ – flexibility effect, lg -landing gear, ie & oe – inner & outer elevon, ge – ground effect

3.8 Control Power Plants

During liftoff SITVC system will provide the primary pitch & yaw control system and RCS will provide the roll control force. When the dynamic pressure increases fin tip will be effective so the SITVC requirement will come down. Only when the fin tip alone is not sufficient, SITVC will be called for to augment the fin tip system. When the dynamic pressure increases the roll control is planned using the outer elevon differential deflections.

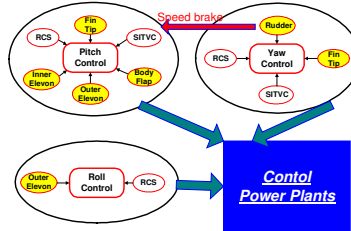


Figure 4 : Control power plant

The fin deflection combination for control is selected such that all four fins are deflected for pitch and yaw control without roll. The control sharing logic between Fins and SITVC is considered such that there is a smooth switching of control from SITVC to FTC during the initial lift off phase. The actuator dynamics for Fin & SITVC actuator are modelled as second order system.

During the low dynamic pressure regime ($<2\text{kPa}$) RCS is used for pitch, yaw and roll control. When the dynamic pressure exceeds 2kPa (descent phase) aerodynamic control surfaces of WBRV will provide the control force. Since the vehicle has a large pitching moment during descent phase and in order to control the vehicle most of the control surfaces are capable for correcting in pitch plane. Body flap, elevon (inner & outer) and rudders acting as speed brake are used for pitch control. For controlling in yaw plane rudders are used which are effective when the angle of attack is less than 10° and dynamic pressure greater than 2kPa . The differential deflection of the outer elevons will provide the roll control force.

3.9 Navigation

The NGC configuration consists of two types of sensors that are used for the ascent and reentry phases of the mission. The two sensors are the Flush Air Data system (FADS) and Inertial Navigation System (INS). FADS consists of matrix of flush mounted pressure tapings located in and around nose cone of the vehicle which measures the static pressure at these orifices and presented to an estimation algorithm which will compute the air data parameters in an onboard computer. FADS provides the air data parameters namely Mach number, angle of attack, sideslip and dynamic pressure. Inertial Navigation System (INS) consists of gyros, and accelerometers, which provide the information of the sensed angular rates and acceleration experienced by the vehicle. The sensed position, velocity, lateral acceleration, angular velocity and attitude angles are derived from the acceleration and angular velocity computed from vehicle dynamics. Computed angular velocity is subjected to sensor dynamics to generate the sensed angular velocity. The differential equation for quaternion is integrated using the sensed angular velocity and the quaternion parameters so obtained are used to derive the sensed attitude angles. INS system is planned for the ascent phase and a combination of FADS and INS for the re entry phase.

3.10 Guidance

For the atmospheric phase of ascent flight open loop mode of guidance will be followed. Guidance will generate the vehicle steering angles (pitch, yaw and roll). In open loop guidance these steering angles are generated a priori through trajectory optimisation and stored as input to the flight simulation. Here steering angles vs time/altitude are stored as input data. Instantaneous steering angles are computed based on time or altitude as required by the mission. In closed loop guidance, the steering angles are computed at every instant of flight based on the vehicle state and target conditions. For re-entry vehicles the guidance commands are expressed in terms of angle of attack and bank angles. These angles will be computed by the closed loop guidance system based on the g-loads, heat levels, downrange, cross range and the terminal landing conditions. These commands are issued to autopilot.

3.11 Autopilot

The commands to control actuators are generated using the commanded attitude computed by guidance algorithm and the sensed attitude, sensed angular velocity and lateral acceleration computed by navigation algorithms. Attitude input to control law is obtained by computing the error from commanded attitude and sensed attitude and then multiplying with error gain. The output of autopilot is shared between the different control plant such as Fin tip control system, RCS, SITVC and the aerodynamic control depending on the control sharing logic adopted for the mission. The actuator requirements depend on the dynamic performance requirements of flight control and estimated hinge moment coefficients. Here a second order dynamic model is considered for the actuator system.

4. Results and Discussions

Flight simulations of a sub-orbital Winged Body Re-entry Vehicle (WBRV) were carried out considering a solid booster of nearly 9 ton propellant loading. The WBRV will be boosted to hypersonic Mach number of about 6. The reference trajectory of the vehicle is generated using the point-mass trajectory optimization software and it is taken for the open loop guidance command generation. The trajectory of the vehicle is designed such that first there is a vertical rise to clear the launch pad and then the vehicle is steered to get maximum Mach number at the time of booster burn out. WBRV flight simulation results are compared with the reference trajectory parameters. The comparison of the altitude profile for ascent phase is shown in **figure 5**. The results are closely matched with the reference trajectory.

A typical wind profile up to 80 km is considered along with the reference trajectory for the simulation to assess the control requirements, mission critical flight parameters for liftoff to touch down flight phases. The typical results are presented.

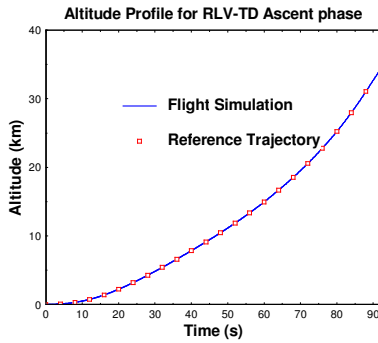


Figure 5 : Comparison of simulation Vs reference trajectory

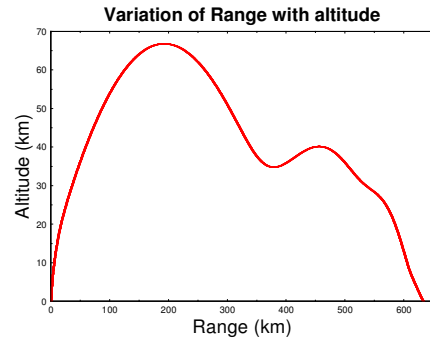


Figure 6 : Altitude Vs Range variation

Figure 6 shows the maximum range covered during the mission is about 650km. There are no intentional cross range maneuvers planned for the present WBRV mission.

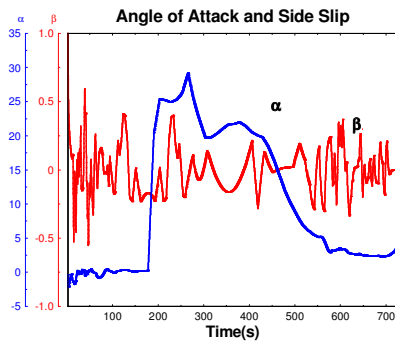


Figure 7 : Angle of attack and Sideslip

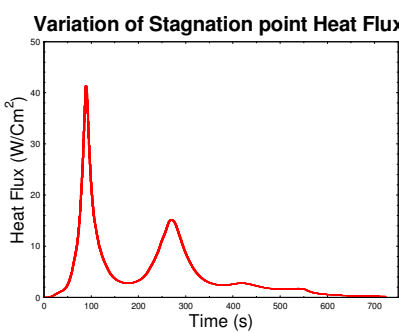


Figure 8 : Nose cap heat flux variation

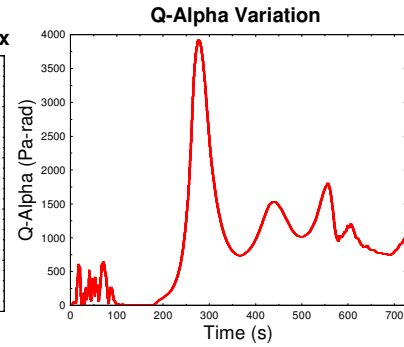


Figure 9 : Q alpha variation

Angle of attack and sideslip variation from liftoff to touch down is shown in **figure 7**. During the ascent phase the vehicle flies a low angle of attack trajectory and angle of attack increases to about 29° during the descent phase. The sideslip angle varies with in the range of 0.5° . **Figure 8** depicts the stagnation point heat flux at WBRV nose cap and maximum heat flux is about 42W/cm^2 during ascent phase and 16W/cm^2 during the descent phase. For the typical wind considered, **figure 9** shows that the maximum Q -alpha for the ascent phase is about 700Pa-rad and descent phase is about 4000Pa-rad .

Maximum fin deflection during ascent phase is about 8deg for the typical wind profile considered. **Figure 10** shows the fin deflection sensitivity with wind.

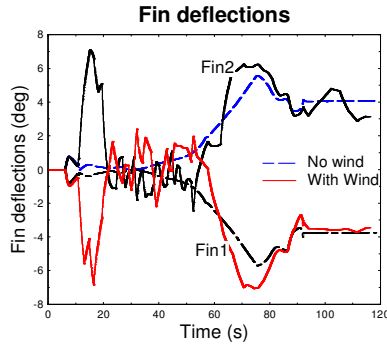


Figure 10 : Fin deflections

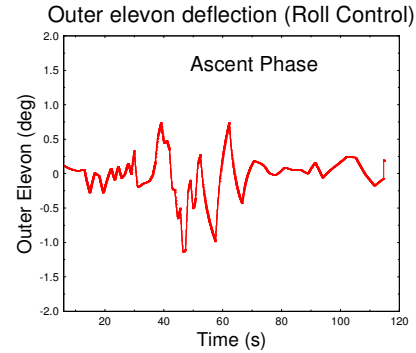


Figure 11 : Outer elevon def. -Ascent phase

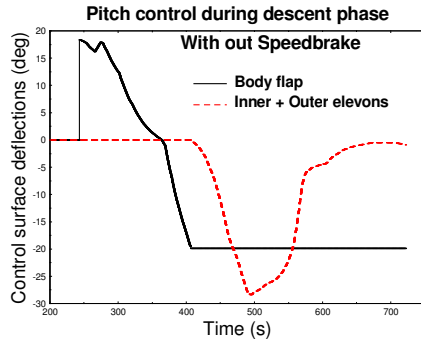


Figure 12 : Body flap & elevon def-Pitch control

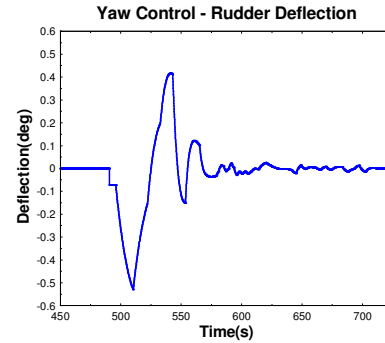


Figure 13 : Rudder deflection - yaw control

Figure 11 shows the outer elevon deflection during ascent phase for roll control. The maximum allowed body flap and elevon deflections are $\pm 20^\circ$ and $\pm 30^\circ$ respectively. The elevon and body flap deflections trailing edge downward is positive and upward is negative. A rudder deflected towards right is positive and towards left is negative (from nose). The pitch control sharing logic for the control surfaces follows the sequence of body flap, inner and outer elevon. Body flap and elevon deflections for pitch control are shown in **figure 12**. **Figure 12** shows that the body flap gets saturated at about 400s and requires nearly the maximum available control deflections for both inner and outer elevons combined. **Figure 13** shows the rudder deflection for yaw control, which is effective at about 490s from liftoff and the maximum deflection is about 0.5° . Rudder requirement is to balance the disturbances due to wind.

Figure 14 shows that the maximum deflection for the outer elevons for roll control is about 0.7deg . Pitch control sharing logic is modified considering the rudder as speedbrake during the Mach number range of 1.2 to 3 to avoid the elevon saturation. The modified control sharing logic during low supersonic regimes is in the sequence of body flap, speedbrake, inner and outer elevons. Two third control of the rudders acting as speed brake is considered during the Mach number range of 1.2 to 3 for pitch control. **Figure 15** shows that the maximum elevon deflection reduces to 10deg and rudder gets saturated. Smooth switch over of the control surface deflections will be considered as a future work for the simulation studies.

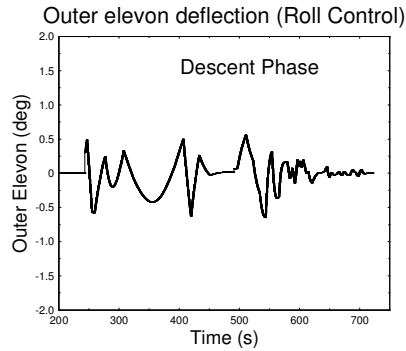


Figure 14 : Outer elevon deflection –Descent phase

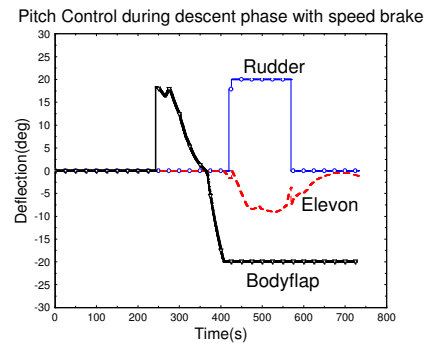


Figure 15 : Pitch control – with Speed brake

5 Conclusions & future work

A six-degree of freedom flight simulation software is developed for winged body reusable launch vehicle using object-oriented approach. Mathematical model and formulation for the ascent and descent phases flight dynamics of reusable launch vehicle is presented. Quaternion approach is used for representing the attitude dynamics of the vehicle. Earth is modeled as a rotating oblate spheroid. WBRV non-linear aerodynamic models were developed based on look up tables obtained from wind tunnel tests and CFD analysis. These aerodynamic coefficients are linearly interpolated for the current flight conditions. Simplified dynamic models were incorporated for the sensors and actuators. All these models are represented with different class architecture along with a user interface to handle the input and output parameters. Flight simulation was done for a sub-orbital Winged Body Re-entry Vehicle from liftoff to touch down. Important flight trajectory and mission critical parameters and the control requirement are presented. To make the simulation software a versatile and general simulation tool it will be extended in terms of friendly user interface, and this is in progress.

Acknowledgement

The authors wish to place on record their sincere gratitude to Shri E Janardhana Ex-Deputy Director, Launch Vehicle Design Entity, VSSC, for his vision and inspiration, to materialize this activity. We would like to thank Shri, Jaison Joseph and Shri Aravind Mishra, LVDE VSSC for providing the steering program and autopilot data. We also like to thank Shri M.M Patil, Shri Balram Panjwani & Shri Dhanajaya Rao, LVDE, VSSC for providing the aerodynamic data to complete this work. The authors gratefully acknowledge Shri M.V Dhekane, DH CLD, VSSC for the suggestions after review of the paper.

References

- [1] J.M.Rolfe, K.J.Staples, Flight Simulation, Aerospace series, Cambridge.
- [2] Regan FJ, Reentry vehicle Dynamics, AIAA education series.
- [3] Stoustrup, Bjarne, "The C++ programming language", II edition, Addison-Wesley, 1991.
- [4] Etkin B, Dynamics of Atmospheric flight. John Wiley & Sons Inc. Newyork 1972.
- [5] Cornelisse, JW, Schoyer, HFR and Walker, KF, Rocket Propulsion and Space flight dynamics. Pitman London 1979.
- [6] Joseph M. Cooke et al. NPSNET Flight simulation dynamic modeling using Quaternions. Proceeding of the Symposium on Interactive 3D Graphics 1992.



This page has been purposely left blank